Coupling between plane waves and Bloch waves in photonic crystals with negative refraction

Zhichao Ruan, Min Qiu,* Sanshui Xiao, Sailing He, and Lars Thylén

Joint Research Center of Photonics of the Royal Institute of Technology (Sweden) and Zhejiang University, Zhejiang University, Yu-Quan, 310027 Hangzhou, People's Republic of China

Laboratory of Optics, Photonics and Quantum Electronics, Department of Microelectronics and Information Technology, Royal Institute of Technology (KTH), Electrum 229, 16440 Kista, Sweden

A comprehensive analysis of the coupling coefficients between plane waves in conventional dielectric media and Bloch waves of photonic crystals with effective negative refractions is performed by the layer Korringa-Kohn-Rostoker method. Employing the infinite layers refraction operator, semi-infinite size photonic crystals are considered. Some special coupling properties are discussed. In particular, the strong angular dependence of coupling coefficients is found even for an interface between air ($n=1$) and a photonic crystal with effective refractive index ($n_{\text{eff}}=-1$). Thus, a negative refractive index defined by the radius of a circular equal-frequency contour does not guarantee an isotropic behavior.

I. INTRODUCTION

Recently the subject of negative refractions has inspired a lot of interest in physics for their important potential applications. A well-known example is a negative index material (NIM; also called a left-handed material), which exhibits a negative refractive index due to the simultaneous negative permeability and permittivity.[1–8] It has been proposed that subdiffraction-limited optical resolution can be achieved with a perfect lens—a planar slab of a NIM.[9] Another equally important aspect of negative refraction is that under certain conditions, photonic crystals (PhCs) can also refract light with a negative refraction angle.[10–18] It has been just recently experimentally demonstrated at the microwave wavelengths,[19,20] and at the optical communication wavelengths.[21] The subwavelength resolution of an image due to the negative refraction of PhCs has been demonstrated experimentally.[22]

It was shown theoretically by Notomi[11] that in a strongly modulated photonic crystal, the contours of equal-frequency surfaces (EFS's) in the vicinity of the photonic band gap might become circular, which are similar to that of a conventional isotropic dielectric material. Therefore, an effective refractive index of the PhC for all angles can be defined as that of the conventional material. It should be noted that the optical property of a photonic crystal with effective negative refractive index $n_{\text{eff}}=-1$ is different from that of a negative index material with refractive index $n=-1$. For a NIM with $n=-1$, light can go through an air-NIM interface without reflection.[9] One may observe a different behavior at an interface between air and a photonic crystal with $n_{\text{eff}}=-1$. Thus, a detailed theoretical study of light coupling between conventional dielectric materials and photonic crystals is important to estimate the validity of the physical model that a PhC with an effective negative refractive index can be treated as an isotropic NIM.

The scattering problems of the periodical structure have been studied by many authors, and many numerical methods have been applied to these problems in the optical field and the quantum field alike, e.g., Refs. 23–27. In the present paper, the versatile layer-KKR (Korringa-Kohn-Rostoker) method[17,28–32] is used to calculate the coupling coefficients between plane waves in conventional dielectric media and Bloch waves of photonic crystals with effective negative refractions. The layer-KKR method is a rigorous method based on the expansion of cylindrical harmonics for the two-dimensional structure (or spherical harmonics for the three-dimensional), and thus is very suitable for cylindrical (or spherical) inclusions. After introducing the scattering matrices of the monolayer in a photonic crystal, it can obtain eigenstates (i.e., photonic band structures) of the PhC, or compute the transmissions and reflections for the PhC slab. The photonic crystals studied in the present paper all exhibit negative refraction properties at the frequency range of interests. The influence of interface orientations and mode symmetries to the coupling efficiency is also addressed.

II. NUMERICAL METHOD

A schematic diagram of the structures studied in the present paper is shown in Fig. 1. Assume a plane wave incident upon the semi-infinite photonic crystal with a wave vector $\mathbf{k}=(k_x, \gamma_0)$ perpendicular to the axes of the cylinders. Each diffracted wave outside the grating, including the propagating or evanescent components, can be expressed by the plane wave with the wave vector $\mathbf{k}_p^{\pm}$,

$$\mathbf{k}_p^{\pm} = (\alpha_p, \pm \gamma_p),$$

$$\alpha_p = k_x + 2\pi p/d, \quad \gamma_p = \sqrt{k_b^2 - \alpha_p^2}, \quad (1)$$

where the integer p denotes the diffraction orders, d is the period in the x direction, and k_b is the wave number in the background dielectric media. When γ_p is real (or purely imaginary), the superscripts $+$ and $-$ denote the components propagating (or decreasing) along $+y$ and $-y$ directions, respectively. And $\mathbf{u}_{\text{inc}}$ denotes the column vector composed of the Fourier coefficients of the incident light. In the layer-KKR method, the field amplitudes at the jth and $(j+1)$th interfaces can be related by[17]
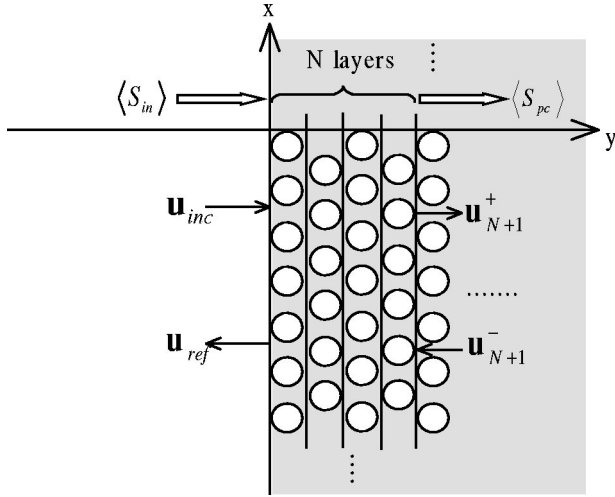
FIG. 1. The semi-infinite PhC structure consists of the front N layers and the rear semi-infinite layers. $\mathbf{u}_{N+1}^{\pm}$ denotes the field amplitude at the $N+1$ interface (between the front N layers and the rear semi-infinity system).

$$\begin{bmatrix} \mathbf{u}_{j+1}^{+} \\ \mathbf{u}_{j}^{-} \end{bmatrix} = \begin{bmatrix} \widetilde{\mathbf{T}}^{++} & \widetilde{\mathbf{R}}^{-+} \\ \widetilde{\mathbf{R}}^{+-} & \widetilde{\mathbf{T}}^{--} \end{bmatrix} \begin{bmatrix} \mathbf{u}_{j}^{+} \\ \mathbf{u}_{j+1}^{-} \end{bmatrix}, \quad (2)$$

where $\mathbf{u}_{j}^{\pm}$ is the column vector composed of the Fouier coefficients of the forward $(+)$ and backward $(-)$ propagating mode at the jth interface, and $\widetilde{\mathbf{T}}$ and $\widetilde{\mathbf{R}}$ represent the transmission and reflection matrices characterizing the diffraction properties of the grating (between the two neighboring interfaces) to the incident plane wave with the wave vector $\mathbf{k}$. The scattering matrices $\widetilde{\mathbf{T}}$ and $\widetilde{\mathbf{R}}$ for a monolayer can be directly calculated with a KKR method based on the expansion of cylindrical harmonics.[32]

Using the above transmission and reflection matrices of monolayer, the transmission matrix $\widetilde{\mathbf{T}}_{N}^{++}$ and the reflection matrix $\widetilde{\mathbf{R}}_{N}^{-+}$ of N layers can also be obtained by a stable recursive formula (based on the scattering scheme in Ref. 32). To solve a general case that there are two different background dielectric materials at two sides of the interface, a scattering matrix of the homogenous plate[29,30] can be added to $\widetilde{\mathbf{T}}_{N}^{++}$ and $\widetilde{\mathbf{R}}_{N}^{-+}$. For the Bloch wave propagating through the monolayer in PhC, the fields at each interface differ only by a multiplicative phase shift. The eigenstate $([\mathbf{g}_{+}^{T}, \mathbf{g}_{-}^{T}]^{T})$ with the eigenvalue μ at each interface can be computed by the transmission and reflection matrices of monolayer (see Appendix A). Following the treatment in Ref. 33, the important reflection matrix $\widetilde{\mathbf{R}}_{\infty}^{+-}$ for the semi-infinite space with an infinite number of grating layers can also be deduced (see Appendix B).

For the semi-infinite PhC considered in Fig. 1, it can also be treated as the composing of the front N layers and the rear semi-infinite layers. Considering that the dielectric material outside PhC may be different from the background material of PhC, the interface between the conventional dielectric material and the PhC is chosen to be normal to all the inclusions

in the first layer. To obtain the coupling coefficient between the plane wave in the conventional dielectric material and the Bloch wave in the photonic crystal, one only needs to calculate the field travelling through a few layers after the dielectric-PhC interface, where the evanescent forward mode has completely decayed, e.g., the field is a superposition of the pure bulk guided mode. At the $N+1$ interface (between the front N layers and the rear semi-infinity system, see Fig. 1), one can apply Eq. (2) to obtain

$$\mathbf{u}_{N+1}^{+} = \widetilde{\mathbf{T}}_{N}^{++} \mathbf{u}_{\text{inc}} + \widetilde{\mathbf{R}}_{N}^{-+} \mathbf{u}_{N+1}^{-}, \quad (3a)$$

$$\mathbf{u}_{N+1}^{-} = \widetilde{\mathbf{R}}_{\infty}^{+-} \mathbf{u}_{N+1}^{+}. \quad (3b)$$

In the above equation, $\mathbf{u}_{\text{inc}}$ is the column vector composed of the Fourier coefficients of the incident light, and $\widetilde{\mathbf{R}}_{N}^{-+}$, $\widetilde{\mathbf{T}}_{N}^{++}$ are the transmission and reflection matrices for the front N layers. For there is no backward wave in the semi-infinity system, $\mathbf{u}_{N+1}^{-}$ has only the contribution from the $\mathbf{u}_{N+1}^{+}$ in Eq. (3b). The field excited by the incident field at the Nth interface is then obtained by

$$\begin{bmatrix} \mathbf{u}_{N+1}^{+} \\ \mathbf{u}_{N+1}^{-} \end{bmatrix} = \begin{bmatrix} \mathbf{I} \\ \widetilde{\mathbf{R}}_{\infty}^{+-} \end{bmatrix} \left(\mathbf{I} - \widetilde{\mathbf{R}}_{N}^{-+} \widetilde{\mathbf{R}}_{\infty}^{+-} \right)^{-1} \widetilde{\mathbf{T}}_{N}^{++} \mathbf{u}_{\text{inc}}. \quad (4)$$

And the reflectance can be easily obtained from

$$\mathbf{u}_{\text{ref}} = \widetilde{\mathbf{R}}_{N}^{+-} \mathbf{u}_{\text{inc}} + \widetilde{\mathbf{T}}_{N}^{--} \mathbf{u}_{N+1}^{-}, \quad (5)$$

where $\mathbf{u}_{\text{ref}}$ is the column vector composed of the Fouier coefficients of different reflection orders. Though reflected waves with high diffraction orders (p) are possible, many of them are evanescent waves. Here we only consider those propagating reflected waves (i.e., when γ_{p} is real).

The portion of each eigenstate in the excited field can be expressed by the following formula:

$$\eta_{\mu} = \frac{\langle \mathbf{g} | \mathbf{u} \rangle^{2}}{\langle \mathbf{g} | \mathbf{g} \rangle \langle \mathbf{u} | \mathbf{u} \rangle}, \quad (6)$$

where $\mathbf{g}$ and $\mathbf{u}$ denote the column vector of the eigenstate $([\mathbf{g}_{+}^{T}, \mathbf{g}_{-}^{T}]^{T})$ with the eigenvalue μ and the excited field $([\mathbf{u}_{N+1}^{+}{}^{T}, \mathbf{u}_{N+1}^{-}{}^{T}]^{T})$ of the PhC, respectively. In the cases that the incident wave can exit only one eigenstate, the portion of the eigenstate within the excited field should be 100%, i.e., $\eta_{\mu} = 1$. It is shown that in our numerical examples, the calculated result η_{μ} is almost 100% with an error less than 10^{-6}, even though only 16 layers are used in the calculations.

After obtaining the field at the $(N+1)$th interface, where N can be arbitrary as long as N is big enough so that evanescent forward waves have decayed significantly after traveling through these N layers [i.e., the field at the $(N+1)$th interface is simply a superposition of pure Bloch modes], the time-average energy flux $\langle S_{pc} \rangle$ along the y-direction can be easily calculated.[33] The wave coupling coefficient between the dielectric medium and the photonic crystal can be defined in the following formula:
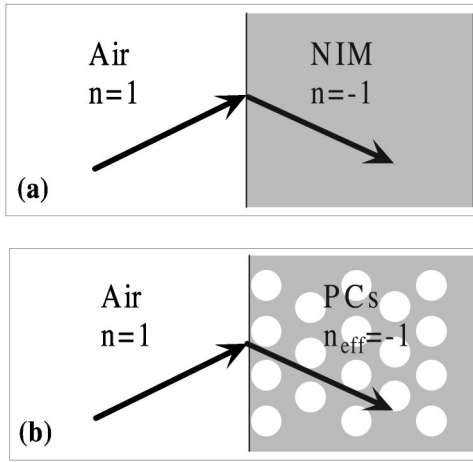
FIG. 2. Schematic diagram of light propagation: (a) from air to the negative index material with $n=-1$ (b) from the air to the PhC with an effective refractive index $n_{eff}=-1$.

$$c = \frac{\langle S_{pc} \rangle}{\langle S_{in} \rangle}, \qquad (7)$$

where $\langle S_{pc} \rangle$ and $\langle S_{in} \rangle$ represent the time-average power fluxes along the y direction of the excited field and the incident field, respectively.

III. COUPLING EFFICIENCY FOR PHOTONIC CRYSTALS WITH NEGATIVE REFRACTION

We first consider a 2D photonic crystal with a triangular lattice of air holes. As assumed in Ref. 11, the background material is chosen as GaAs ($n=3.6$) and the radius of the air holes is $0.4a$, where a is the lattice constant. It has been shown that under the TM polarization (only the electric field along the z direction), the shape of the EFS is almost circular

at the second band for a frequency window between $\omega = 0.29$ and $0.34(2\pi c/a)$, which is similar to that of a conventional isotropic dielectric material. Thus an effective refractive index can be defined as that for the dielectric material. On the other hand, the propagation direction of light beams in any medium is given by the energy velocity vector. It has been proved that in PhCs, as for homogeneous materials, the energy velocity vector equals to the group velocity vector $\mathbf{v}_g$.[34,35] By definition the group velocity vector $\mathbf{v}_g = \nabla_{\mathbf{k}} \omega$ is always oriented perpendicular to the EFS in the direction along which the frequency ω is increasing. For the second band of the PhC, the group velocity vector is pointed inward from the EFS, which means a negative refraction.[11] Therefore, an effective negative refractive index can be obtained, in particular, $n_{eff}=-1$ at the frequency $\omega=0.31(2\pi c/a)$.

It is known that there is no reflection at the interface between a negative index material $n=-1$ and a conventional dielectric material $n=1$ (Ref. 9) [see Fig. 2(a)]. In other words, the coupling coefficient at any incident angle is always 100%. However, for the air-PhC interface with the photonic crystal of $n_{eff}=-1$ [see Fig. 2(b)], results are quite different. Employing the layers-KKR method given in the preceding section, the coupling coefficients are shown in Fig. 3 for two common interfaces, (a1) normal to the $\Gamma-M$ direction, and (b1) normal to the $\Gamma-K$ direction, respectively, at the frequency $\omega=0.31(2\pi c/a)$. Several significant features can be seen in Fig. 3. First, the coupling coefficient is never close to 100%. For the interface normal to the Γ-M direction, the maximum coupling coefficient is only about 65%. The coupling coefficient actually drops down to zero when the incident angle increases. Second, the coupling coefficient at the interface normal to the Γ-K direction is always less than 1%. For the normal incident, the coupling coefficient is zero, that is, the normal incident plane wave cannot excite the Bloch wave in the PhC. At larger angles the coupling coefficient increases a little bit, reaches the first maximum at about incident angle 30° (i.e., along the Γ-M direction), and
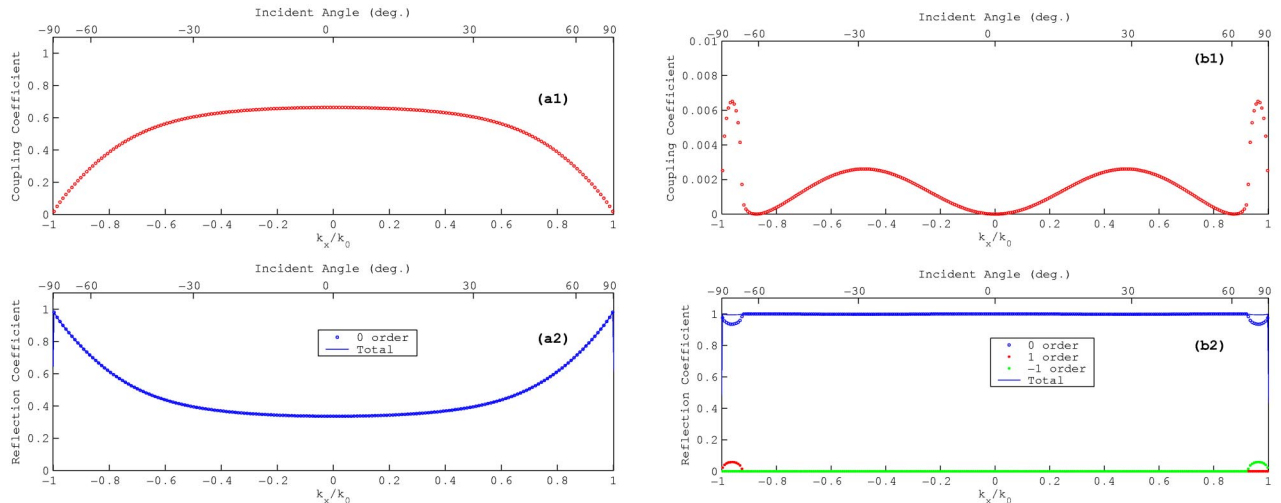
FIG. 3. (Color online) For air-PhC interfaces, the coupling coefficients at the different interface (a1) normal to the Γ-M direction, and (b1) normal to the Γ-K direction, at the frequency $\omega=0.31(2\pi c/a)$. The reflection coefficients are plotted in (a2) and (b2) for these two case, respectively. The total line in (a2) and (b2) denotes the sum of all propagation order reflectance. Here k_x is the x component of the incident wave vector and k_0 is the wave number in the vacuum.
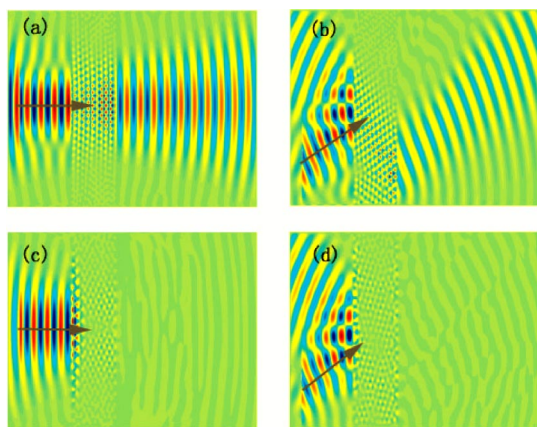
FIG. 4. (Color online) The stable field (E_z) distribution of incident Gaussian beams at the frequency $\omega=0.31(2\pi c/a)$. (a) and (b) are for the surface interfaces of the PhC slab normal to the Γ-M direction, and (c) and (d) are for the surface interfaces normal to the Γ-K direction. The arrows indicate the incident angle, $\phi=0°$ in (a) and (c) and $\phi=30°$ in (b) and (d).

the second maximum for the larger angle near 75°.

The reflection coefficients for each case can also be obtained from Eq. (5), and are plotted in Figs. 3(a2) and 3(b2), respectively. It is interesting to notice that, for both cases, most of the reflection is from the zeroth order of light, and the contribution from high-order light is negligible.

To illustrate the previous results, several simulations are made by using a finite-difference time-domain (FDTD) method.[36] A Gaussian beam with the frequency ω $=0.31(2\pi c/a)$ is launched with a certain incident angle ϕ into the different PhC slabs, where the surface interfaces are normal to the Γ-M direction (12 PhC layers) or the Γ-K direction (20 PhC layers). Figure 4 shows the stable field distribution (E_z) for the Gaussian beam with different incident angles ($\phi=0°$ and 30°). The transmission can be estimated from the FDTD simulations by calculating the energy flux along the y direction. In the case of the surface interface normal to the Γ-M direction, the transmission is 19.04% for $\phi=0°$ and 18.91% for $\phi=30°$. However, it is clear that the beam is very difficult to propagate through the PhC slab with

the surface interface normal to the Γ-K direction. The transmission is only 1.5×10^{-6} for $\phi=0°$ and 0.018% for $\phi=30°$. These are in agreement with our previous calculations by the layer-KKR method, though the values are different since only a finite-size PhC slab is considered here.

The phenomena of the above highly angular dependence on the coupling coefficient can be explained by the symmetry mismatch between modes. On the high symmetric axes in the Brillouin zone, the symmetry of the bulk Bloch modes can be classified by the group theory.[35,37] The group theory tells that the eigenfunction is an irreducible representation of the point group. For **k** along the Γ-M direction or along the Γ-K direction, modes have a C_{1h} symmetry, which corresponds to two different irreducible representations.[35] It means that the field can be classified as an even or odd symmetry with respect to the mirror plane along the wave vector. By the plane-wave expansion approach, the field distributions of the bulk modes at the frequency $\omega=0.31(2\pi c/a)$, with the Bloch wave vectors **k** in the Γ-M direction and the Γ-K direction are shown in Fig. 5. It is clear that the bulk mode has even symmetry for the Bloch wave vectors **k** in the Γ-M direction, and odd symmetry for the Bloch wave vectors **k** in the Γ-K direction. Since the external plane wave at normal incidence is of even symmetry, only the Bloch waves with an even symmetry can be excited.[16,37,38] Due to this symmetry mismatch, the coupling coefficient at the interface normal to the Γ-K direction is zero at the normal incidence and always small at other near incident angles [see Fig. 3(b1)]. The maximal coupling coefficient obtained at nearly $\pm30°$ incident angle can also be easily explained if we take into account that the wave vector for this excited Bloch wave is nearly at the Γ-M direction.

In Fig. 3(b1), the coupling coefficient maximum at large angles (60°–90°, i.e., $\sqrt{3}/2<k_x/k_0<1$) is mainly due to the influence of neighboring Brillouin zones. The equal-frequency contours at the frequency $\omega=0.31(2\pi c/a)$ are shown in Fig. 6. One can find that there is a region (between the dotted lines), in which the transverse wave vector along the interface direction crosses the equal-frequency contours in the neighboring Brillouin zones. It is known that the parallel component of the wave vector should be conserved. For $\sqrt{3}/2<k_x/k_0<1$, the wave vector of the Bloch wave in the
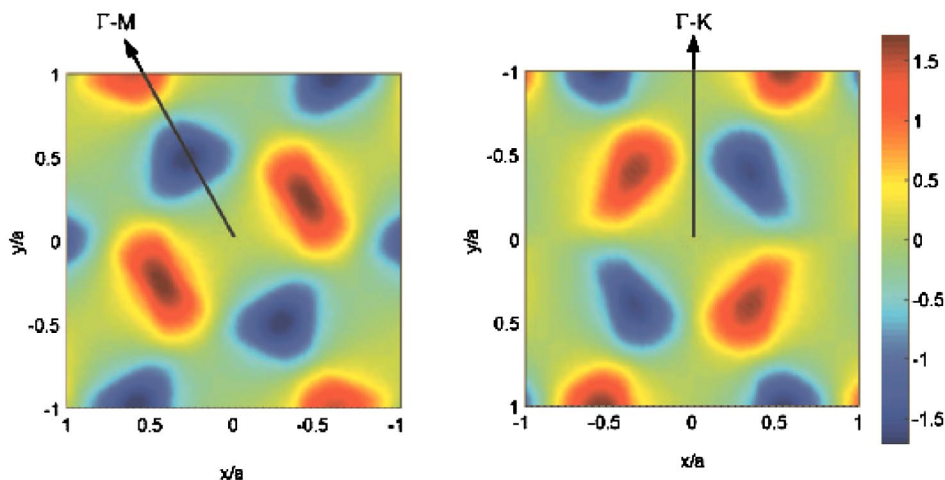
FIG. 5. (Color online) The E_z field distribution of the bulk modes of the photonic crystal at the frequency $\omega=0.31(2\pi c/a)$, where (a) corresponds to the Bloch wave vector **k** at the Γ-M direction, and (b) corresponds to **k** at the Γ-K direction.
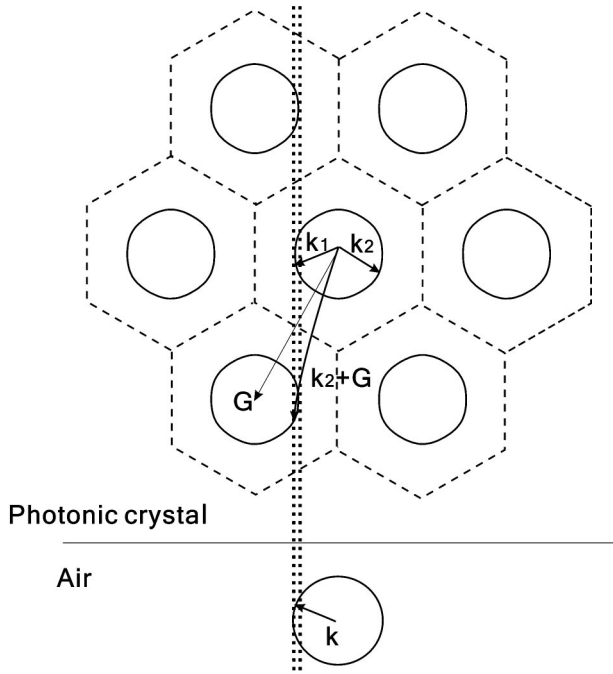
FIG. 6. The equal frequency surface plot for the frequency ω $=0.31(2\pi c/a)$. The plane wave **k** is incident on the interface normal to the Γ-K direction. For the larger incident angles (i.e., the wave vector **k** in the region of the dotted line), the plane wave can excite Bloch waves in PhC with the Bloch wave vectors, $\mathbf{k}_1$ and $\mathbf{k}_2$. Here **G** is the reciprocal lattice vector.

PhC is allowed not only in the first Brillouin zone ($\mathbf{k}_1$), but also in the other Brillouin zones (e.g., $\mathbf{k}_2$). This accounts for the coupling enhancement for $\sqrt{3}/2 < k_x/k_0 < 1$.

For further insight on the coupling another example of a triangular photonic crystal is studied. The photonic crystal consists of the triangular lattice of air-holes with the radius $r=0.4a$ in the background material $n=3.24$. The band structure for the TM mode and the equal-frequency surface have been given in Ref. 12. For the TM mode at the frequency photonic crystal is quite different from that between two conventional isotropic materials. The distinction of the coupling mainly arises from the characteristics of Bloch waves in the photonic crystal (e.g., the eigenstate symmetry and the exciting of high-order Bloch modes). It also means that the equal-frequency surface can define the propagation direction in the photonic crystal, but not guarantee that the optical property of the photonic crystal can be $\omega=0.325(2\pi c/a)$, the resulted effective refractive index is $n_{\text{eff}}=-0.73$.

The dielectric medium outside the PhC is the same as the background material of the PhC. Figures 7(a1) and 7(b1) show the calculated coupling coefficients against the incident angle (solid lines, case A). Figure 7(a1) also gives the coupling coefficients between two conventional isotropic dielectric media with $n=3.24$ and $n=0.73$, calculated by the Fresnel transmission formulas (dashed-dotted lines, case B). Similar as the previous example, the coupling coefficient is quite different for two interfaces. For the interface normal to the Γ-M direction, the coupling coefficient of the case A is largely enhanced compared to that of case B. The maximum coupling here is about 89%, while the value is only 60% for

the dielectric-dielectric coupling. The coupling coefficient rapidly drops down when the incident angle increases. When the incident angle is larger than $13°$, the total internal reflection happens. The coupling coefficient is then zero. For even larger incident angles ($49°$), the wave can then couple with the high-order Bloch waves[12] outside the first Brillouin zone, though the maximal coupling coefficient is only about 20%. On the other hand, the coupling coefficient at the interface normal to the Γ-K direction [Fig. 7(b1)] has a very strange behavior. For small incident angles inside the first Brillouin zone, the coupling coefficient is almost zero due to the mode symmetry mismatch discussed above. At the larger incident angles the coupling coefficient becomes much larger and also obtains the maximal at about $\pm 30°$ incident angle, due to the incident wave vector being nearly along the Γ-M direction. Figures 7(a2) and 7(b2) show the reflectance for the two different cases. It can be seen that the contribution from high order reflection is significant, owing to a large incident plane wave vector **k** (the material index here is $n=3.24$).

IV. CONCLUSION

In conclusion, a comprehensive analysis of the coupling coefficients between plane waves in conventional dielectric media and the Bloch waves of photonic crystals with negative refractions are performed by the layer-KKR method. It is found that the coupling coefficient is highly angular dependent even for an interface between air ($n=1$) and a photonic crystal with effective refractive index ($n_{\text{eff}}=-1$). Therefore, even if the photonic crystal has an effective negative refractive index well defined from the equal frequency contours, the coupling between the plane wave in the dielectric material and the Bloch wave in the photonic crystal is quite different from that between two conventional isotropic materials. The distinction of the coupling mainly arises from the characteristics of Bloch waves in the photonic crystal (e.g. the eigenstate symmetry and the exciting of high-order Bloch modes). It also means that the equal-frequency surface can define the propagation direction in the photonic crystal, but not guarantee that the optical property of the photonic crystal can be the same as that of a conventional dielectric material.

ACKNOWLEDGMENTS

APPENDIX A: THE EIGENSTATES OF PHOTONIC CRYSTALS

To obtain the eigenstates, only a translation operator is required to directly describe the relation of the field at the two interfaces of monolayer, which can be derived from above scattering matrices in Eq. (2),
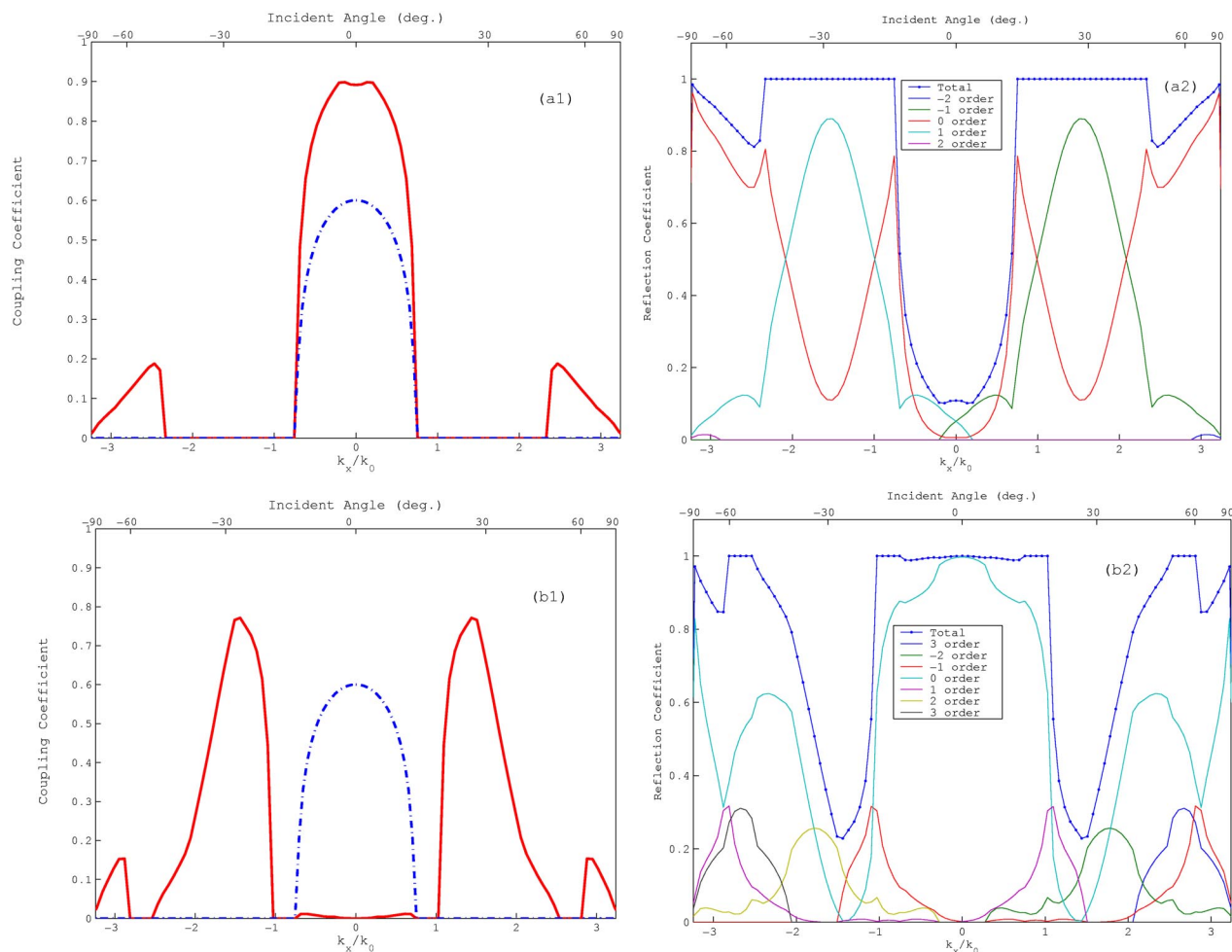
FIG. 7. (Color online) The calculated coupling coefficients (solid lines) and the reflection coefficients for interfaces between the dielectric medium ($n=3.24$) and the photonic crystal ($n_{\text{eff}}=-0.73$) at the frequency $\omega=0.325(2\pi c/a)$. The interfaces are (a1) normal to the $\Gamma-M$ direction, and (b1) normal to the $\Gamma-K$ direction. The dashed-dotted lines are the coupling coefficients between two conventional isotropic dielectric media with $n=3.24$ and $n=0.73$, respectively, calculated by the Fresnel transmission formulas. The reflection coefficients are plotted in (a2) and (b2) for these two cases, respectively. The total line in (a2) and (b2) denotes the sum of all propagation order reflectance.

$$\begin{bmatrix} \mathbf{u}_{j+1}^{+} \\ \mathbf{u}_{j+1}^{-} \end{bmatrix} = \mathcal{T} \begin{bmatrix} \mathbf{u}_{j}^{+} \\ \mathbf{u}_{j}^{-} \end{bmatrix}, \tag{A1}$$

where the monolayer translation operator is given by

$$\mathcal{T} = \begin{bmatrix} \widetilde{\mathbf{T}}^{++} - \widetilde{\mathbf{R}}^{-+}(\widetilde{\mathbf{T}}^{--})^{-1}\widetilde{\mathbf{R}}^{+-} & \widetilde{\mathbf{R}}^{-+}(\widetilde{\mathbf{T}}^{--})^{-1} \\ -(\widetilde{\mathbf{T}}^{--})^{-1}\widetilde{\mathbf{R}}^{+-} & (\widetilde{\mathbf{T}}^{--})^{-1} \end{bmatrix}. \tag{A2}$$

For the Bloch wave propagating through a monolayer in PhC, the fields between layers differ only by a multiplicative phase shift. Therefore, under the Bloch condition the following eigenvalue equation between grating layers can be formed:

$$\mathcal{T} \begin{bmatrix} \mathbf{g}_{+} \\ \mathbf{g}_{-} \end{bmatrix} = \mu \begin{bmatrix} \mathbf{g}_{+} \\ \mathbf{g}_{-} \end{bmatrix}, \tag{A3}$$

where μ is the phase shift and

$$\begin{bmatrix} \mathbf{g}_{+} \\ \mathbf{g}_{-} \end{bmatrix}$$

is the eigenvector of the Bloch state. The eigenvalue μ and the corresponding eigenvector can be obtained by the standard numerical techniques.

APPENDIX B: THE REFLECTION MATRIX $\widetilde{R}_{\infty}^{+-}$ FOR THE SEMI-INFINITE SPACE

The set of eigenvalues and eigenvectors can be grouped into forward and backward propagating states.[33] Since the field of evanescent modes must decay in the propagation direction, the other eigenvectors corresponding to $|\mu| < 1$ (or $|\mu| > 1$) must be the forward (or backward) propagating waves. For Bloch waves in a lossless structure, the eigenvalues must have $|\mu|=1$. To classify the Bloch waves, the group velocity of a Bloch mode in the PhC can be determined from the direction of the time-average energy flux

through the unit cell, where the energy flux $\langle S_{pc} \rangle$ along the y-direction can be obtained from the eigenvectors.[33] If the flux is positive, the Bloch wave is associated with the forward propagation, and vice versa.

For a semi-infinite PhC, there is no rear surface (i.e., the interface between the PhC and another material) to generate the backward propagating modes. All the backward propagating modes are thus generated by the forward propagating modes of the PhC. Let us introduce the matrix $\mathbf{G}_+$, whose columns comprise of the eigenvectors $\mathbf{g}_+$ of the forward modes. In a similar way the matrix $\mathbf{G}_-$ can be obtained for the backward modes. Thus any field at the interface between the gratings can be rewritten as a linear combination of the forward propagating modes,

$$\begin{bmatrix} \mathbf{u}^+ \\ \mathbf{u}^- \end{bmatrix} = \begin{bmatrix} \mathbf{G}_+ \\ \mathbf{G}_- \end{bmatrix} \mathbf{c}, \tag{B1}$$

where $\mathbf{c}$ is the expansion coefficients. Eliminating the coefficients $\mathbf{c}$ yields

$$\mathbf{u}^- = \widetilde{\mathbf{R}}_\infty^{+-} \mathbf{u}^+,$$

where the reflection matrix $\widetilde{\mathbf{R}}_\infty^{+-}$ of the semi-infinite space, a matrix operator connecting the backward propagating modes and the forward propagating modes, can be given by

$$\widetilde{\mathbf{R}}_\infty^{+-} = \mathbf{G}_- \mathbf{G}_+^{-1}. \tag{B2}$$

*Electronic address: min@imit.kth.se

[1] V. G. Veselago, Sov. Phys. Usp. **10**, 509 (1968).

[2] J. Pendry, A. Holden, D. Robbins, and W. Stewart, J. Phys.: Condens. Matter **10**, 4785 (1998).

[3] J. Pendry, Opt. Express **11**, 639 (2003).

[4] D. R. Smith, W. J. Padilla, D. C. Vier, S. C. Nemat-Nasser, and S. Schultz, Phys. Rev. Lett. **84**, 4184 (2000).

[5] R. A. Shelby, D. R. Smith, and S. Schultz, Science **292**, 77 (2001).

[6] M. Bayindir, K. Aydin, E. Ozbay, P. Markos, and C. Soukoulis, Appl. Phys. Lett. **81**, 120 (2002).

[7] C. G. Parazzoli, R. B. Greegor, K. Li, B. E. C. Koltenbah, and M. Tanielian, Phys. Rev. Lett. **90**, 107401 (2003).

[8] A. A. Houck, J. B. Brock, and I. L. Chuang, Phys. Rev. Lett. **90**, 137401 (2003).

[9] J. B. Pendry, Phys. Rev. Lett. **85**, 3966 (2000).

[10] H. Kosaka, T. Kawashima, A. Tomita, M. Notomi, T. Tamamura, T. Sato, and S. Kawakami, Phys. Rev. B **58**, R10 096 (1998).

[11] M. Notomi, Phys. Rev. B **62**, 10 696 (2000).

[12] M. Qiu, L. Thylen, M. Swillo, and B. Jaskorzynska, IEEE J. Sel. Top. Quantum Electron. **9**, 106 (2003).

[13] C. Luo, S. G. Johnson, J. D. Joannopoulos, and J. B. Pendry, Phys. Rev. B **65**, 201104(R) (2002).

[14] C. Luo, S. G. Johnson, J. D. Joannopoulos, and J. B. Pendry, Phys. Rev. B **68**, 045115 (2003).

[15] Z. Y. Li and L. L. Lin, Phys. Rev. B **68**, 245110 (2003).

[16] A. Martinez, H. Miguez, A. Griol, and J. Marti, Phys. Rev. B **69**, 165119 (2004).

[17] S. He, Z. Ruan, L. Chen, and J. Shen, Phys. Rev. B **70**, 115113 (2004).

[18] S. S. Xiao, M. Qiu, Z. C. Ruan, and S. L. He, Appl. Phys. Lett. **85**, 4269 (2004).

[19] P. V. Parimi, W. T. Lu, P. Vodo, and S. Shridar, Nature (London) **426**, 404 (2003).

[20] E. Cubukcu, K. Aydin, E. Ozbay, S. Foteinopoulou, and C. M. Soukoulis, Nature (London) **423**, 604 (2003).

[21] A. Berrier, M. Mulot, M. Swillo, M. Qiu, L. Thylén, A. Talneau, and S. Anand, Phys. Rev. Lett. **93**, 073902 (2004).

[22] E. Cubukcu, K. Aydin, E. Ozbay, S. Foteinopoulou, and C. M. Soukoulis, Phys. Rev. Lett. **91**, 207401 (2003).

[23] F. G. Bass and I. M. Fuks, *Wave Scattering from Statistically Rough Surfaces* (Pergamon, New York,1979).

[24] U. Garibaldi, A. C. Levi, R. Spadacini, and G. E. Tommei, Surf. Sci. **48**, 649 (1975).

[25] N. García, J. Chem. Phys. **67**, 897 (1977).

[26] R. I. Masel, R. P. Merrill, and W. H. Miller, Phys. Rev. B **12**, 5545 (1977).

[27] N. García and N. Cabrera, Phys. Rev. B **18**, 576 (1978).

[28] N. Stefanou, V. Karathanos, and A. Modinos, J. Phys.: Condens. Matter **4**, 7389 (1992).

[29] N. Stefanou, V. Karathanos, and A. Modinos, Comput. Phys. Commun. **113**, 49 (1998).

[30] N. Stefanou, V. Karathanos, and A. Modinos, Comput. Phys. Commun. **132**, 189 (2000).

[31] K. Ohtaka and Y. Tanabe, J. Phys. Soc. Jpn. **65**, 2276 (1996).

[32] K. Ohtaka, T. Ueta, and K. Amemiya, Phys. Rev. B **57**, 2550 (1998).

[33] L. C. Botten, N. A. Nicorovici, R. C. McPhedran, C. Martijn de Sterke, and A. A. Asatryan, Phys. Rev. E **64**, 046603 (2001).

[34] P. Yeh, J. Opt. Soc. Am. **69**, 742 (1979).

[35] K. Sakoda, *Optical Properties of Photonic Crystals*, 1st ed. Springer Series in Optical Sciences 80 (Springer-Verlag, Berlin, 2001).

[36] A. Taflove, *Computational Electrodynamics: The Finite-Difference Time-Domain Method*, 2nd ed. (Artech House, Norwood, 2000).

[37] K. Sakoda, Phys. Rev. B **52**, 7982 (1995).

[38] W. M. Robertson, G. Arjavalingam, R. D. Meade, K. D. Brommer, A. M. Rappe, and J. D. Joannopoulos, Phys. Rev. Lett. **68**, 2023 (1992).